A New Neutron Beam Facility at TSL

Alexander V. Prokofiev [*]**, Olle Byström, Curt Ekström, Volker Ziemann**
The Svedberg Laboratory, Uppsala University
Box 533, S-751 21 Uppsala, Sweden
E-mail: Alexander.Prokofiev@tsl.uu.se

Jan Blomgren, Stephan Pomp, Michael Österlund
Department of Neutron Research, Uppsala University
Box 525, S-751 20 Uppsala, Sweden
E-mail: Jan.Blomgren@tsl.uu.se

Udomrat Tippawan
Fast Neutron Research Facility, Chiang Mai University
50202 Chiang Mai, Thailand
E-mail: Udomrat@fnrf.science.cmu.ac.th

A new quasi-monoenergetic neutron beam facility has been constructed at The Svedberg Laboratory (TSL) in Uppsala, Sweden. Key features include a neutron energy range of 11 to 175 MeV, high fluxes, user flux control, flexible neutron field size and shape, and spacious and easily accessible user area. The first results of the beam characterization measurements are reported.

[*] Speaker

1. Introduction

The interest in high-energy neutrons is rapidly growing, since a number of potential large-scale applications involving fast neutrons are under development, or have been identified. These applications primarily fall into four sectors: nuclear energy and waste [1], medicine [2, 3], flight personnel dosimetry [4], and single-event effects (SEE) on electronics [5, 6].

To satisfy the needs of these applications, monoenergetic neutron beams would be most suitable. In the energy region above about 20 MeV, a truly monoenergetic neutron beam is not feasible in a strict sense. For certain nuclear reactions, however, there is a strong dominance of neutrons in a narrow energy range. Therefore, such neutron sources are often called "quasi-monoenergetic". The most popular neutron production reaction above 20 MeV is ^{7}Li(p,n)^{7}Be. It is used, *e.g.*, at quasi-monoenergetic neutron facilities in Cape Town [7], Davis [8], Louvain-la-Neuve [9], Saitama [10], and Takasaki [11].

There is a long-term experience in high-energy neutron production at The Svedberg Laboratory (TSL). The first neutron facility was built at TSL in the late 1980s [12, 13] and remained in operation until 2003. In 2003-2004, a new facility was constructed. Emphasis was put on high neutron beam intensity in combination with flexibility in energy and neutron field shape.

2. Technical specification

The facility uses the ^{7}Li(p,n)^{7}Be reaction to produce a quasi-monoenergetic neutron beam. Two kinds of beams from the Gustaf Werner cyclotron are used for neutron production: 1) proton beam with energy variable in the 25-180 MeV range, and, 2) beam of H_2^{+} ions with energy of about 13 MeV/A. The energy of the produced peak neutrons is controllable in the 11-175 MeV range.

A drawing of the neutron beam facility is shown in Fig. 1. The proton or H_2^{+} beam is incident on a target of lithium, enriched to 99.99% in ^{7}Li. The available targets are 1, 2, 4, 8.5, and 23.5 mm thick. Proton energy loss in the target amounts to 2-6 MeV depending on the incident beam energy and target thickness. The targets are rectangular in shape, 20x32 mm^2, and are mounted in a remotely controlled
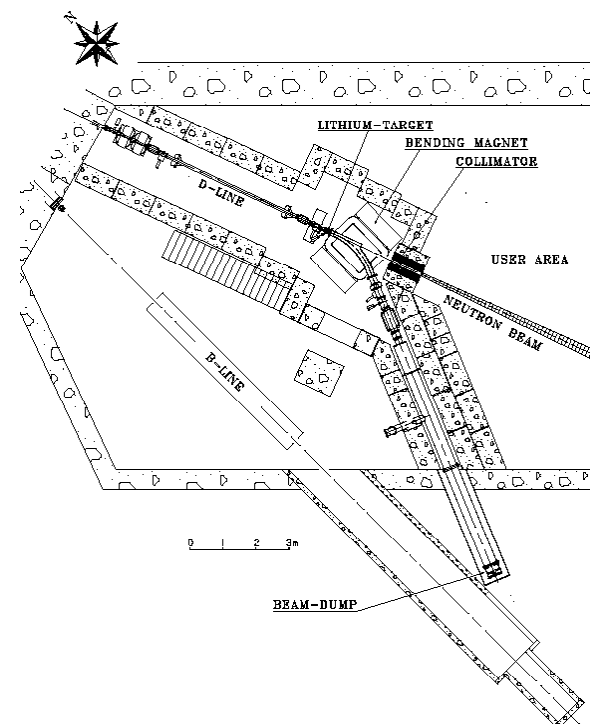
Fig. 1. Drawing of the new neutron beam facility. The neutron beam, produced in the lithium target, continues along the D-line.

water-cooled copper rig. An additional target position contains a fluorescent screen viewed by a TV camera, which is used for beam alignment and focusing. Downstream the target, the proton beam is deflected by a magnet into a 10-m long dumping line, where it is guided onto a heavily shielded water-cooled graphite beam dump.

The neutron beam is formed geometrically by a cylindrically shaped iron collimator block, 50 cm in diameter and 100 cm long, with a hole of variable size and shape. The collimator is surrounded by concrete to form the end wall of the production line towards a user area. Thereby, shielding from the lithium target region is achieved that is sufficient for most experiments. A modular construction of the collimator allows the user to select the size and the shape of the neutron beam. At present, the available collimator openings are 2, 3, 5.5, 10, 15, 20, and 30 cm in diameter. In addition, a quadratically shaped opening of 1 cm^2 is available, which is intended for irradiation of, *e.g.*, a separate electronic component without affecting the rest of an electronic board. Other collimator openings in the 0-30 cm range can be provided upon request. The time needed to change the opening size is typically about 30 min.

The user area extends from 3 to 15 m downstream the lithium target. Positions located closest to the target are used for high-flux irradiation of compact objects, with achievable fluxes about an order of magnitude higher compared to the old TSL neutron facility [12, 13], for the same target thickness, proton energy and current. Remote positions may be used to irradiate large objects, up to 1 m in diameter, e.g., entire computers or aircraft navigation systems. Proton beam currents of up to 10 μA can be used for energies below 100 MeV. Above 100 MeV, the achievable beam current is about a factor of 10 lower. The resulting reduction of the neutron flux can be partly compensated by using thicker lithium targets. The neutron flux can be varied by the user according to the needs of the specific experiment.

The user area, situated at a level of 12 m below the ground, is connected by Ethernet and coaxial cables, about 100 m long, to counting rooms, which are located at the ground level. No time is required for "cooling down" of the user area after irradiation, because the dose rate from residual β- and γ-rays is then only slightly above the natural radiation level.

Two additional irradiation positions, which can be used parasitically with other experiments, are provided closer to the lithium target (see Table I). The increase of the neutron flux at these positions is reached at the expense of limited accessibility, limited size of irradiated objects, lack of standard monitors, and more intense γ-ray background.

Table I. Parasitic irradiation positions.

Position	Distance from the Li target (m)	Angle to the proton beam direction (°)	Gain in the peak neutron flux
PARTY	1.9	1.6	2.5
TUNIS	1.1	7.5	1.7 – 2.2[a]

[a] dependent on the peak neutron energy.

3. Characterization of the facility

Neutron spectra at 0° have been obtained by measuring elastic *np*-scattering with the Medley setup [14-16]. The scattered protons are registered at an angle of 20° relative to the neutron beam. The measured neutron spectra are shown in Fig. 2 for peak energies of 21.8 (a), 46.5 (b), 94.7 (c), and 142.7 MeV (d). In all cases, the spectrum is dominated by a peak situated a few MeV below the energy of the primary protons and comprising about 40% of the total number of neutrons.

Fig. 2 includes a comparison of the measurements with model calculations of the neutron spectra folded with the function that describes the energy resolution in the present experiment. For the three higher energies (Fig. 2b-d), the systematics of Prokofiev *et al.* [17] was employed. For the peak neutron energy of 21.8 MeV, the evaluation of Mashnik *et al.* [18] was used (Fig. 2a). The differential cross-section for high-energy peak neutron production at 0° was obtained by multiplication of the angle-integrated cross-section of the ^{7}Li(p,n)^{7}Be reaction [18] to the "index of forwardness" from the systematics of

Fig. 2. The neutron spectra at 0° for different peak neutron energies (see Table II for incident proton energies and ^{7}Li target thicknesses). Symbols connected by a solid line represent experimental data obtained in the present work. Predictions are shown as dashed lines (see text).

Uwamino *et al.* [19]. The experimental data agree with the calculations except for the low-energy tail region in the 21.8-MeV spectrum where the model overpredicts the yield of neutrons with energies above 5 MeV by about 40%.

Table II summarizes the main features of the measured spectra and the achieved neutron fluxes. The latter have been measured with a monitor based on a thin-film breakdown counter (TFBC) [20]. Another monitoring option is provided by an ionization-chamber monitor (ICM). Both monitors utilize neutron-induced fission of ^{238}U with the cross-section adopted as neutron flux standard [21]. In addition, the neutron flux is indirectly monitored by a Faraday cup, which integrates the current of protons collected at the beam dump. In Table II, γ-ray dose rate in the user area is given as well.

The measured contamination of the neutron beam at the user area, due to interactions of the primary protons with beam transport elements, typically does not exceed 0.05% for peak neutron energies up to 100 MeV and 0.3% for the 174 MeV energy. Such interactions lead to a minor surplus of neutrons in the user area, because charged particles produced near the lithium target and upstream are removed by the deflection magnet. The relative contamination of the
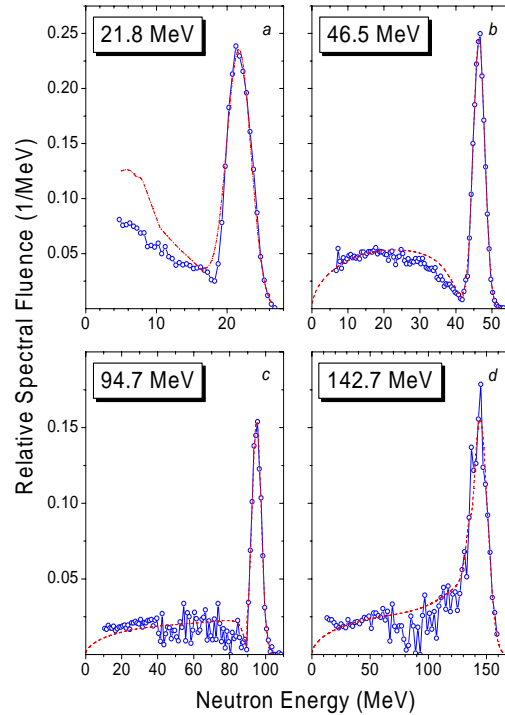
neutron beam by protons with energies above 15 MeV is about 10^{-5} for the peak neutron energy of 95 MeV.

Thermal neutrons were found in the user area, using TFBCs with ^{235}U targets, shielded by a cadmium sheet during a part of the runs. The thermal neutron flux was estimated to be about 1% of the peak neutron flux at 174 MeV energy [22]. This result comes from an ongoing systematic study of the low-energy part of the neutron spectra using TFBCs and different neutron-induced fission reactions.

Figure 3 shows a horizontal beam profile for 142.7-MeV neutrons, measured at a distance of 4.77 m from the lithium target. The measurement was performed by counting neutron-induced SEE in a set of memory chips positioned across the beam [23].
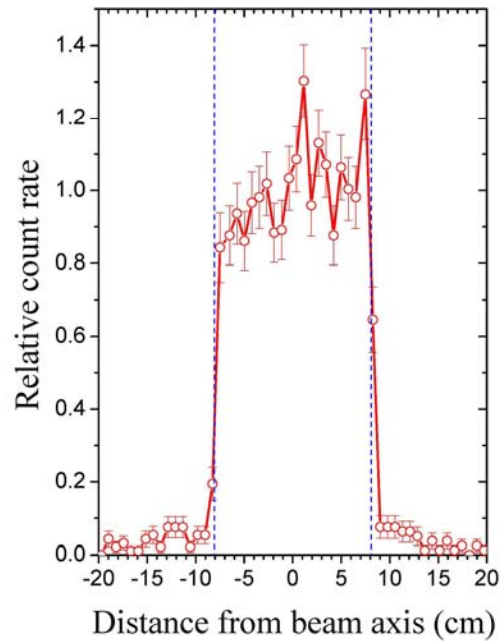

Fig. 3. The horizontal beam profile for 142.7-MeV neutrons, measured at the distance of 4.77 m from the lithium target. Vertical dashed lines represent boundaries of the beam expected from the geometry of the collimator.

4. Summary and outlook

A new neutron beam facility has been constructed at TSL, and it is in frequent operation now (25 weeks during year 2005). The facility is capable of delivering neutrons in the 11-175 MeV range. This makes TSL the only laboratory in the world offering full quasi-monoenergetic neutron testing according to the JESD89 standard [6].

Recently, a neutron field with the peak energy of about 11 MeV has been developed. Processing of neutron spectra at 11 and 174 MeV is in progress. A fast ionization chamber for regular checks of the neutron spectrum is under development [24]. An additional neutron

Table II. Neutron beam parameters.

Proton beam energy (MeV)	^{7}Li target thick-ness (mm)	Proton beam current (μA)	Average energy of peak neutrons (MeV)	Fraction of neutrons in the high-energy peak (%)		Peak neutron flux (10^5 cm^{-2}s^{-1}) a)	γ-ray dose rate (mSv/h) b)
				Meas-ured	Calc-ulated		
24.68 ± 0.04	2	10	21.8	~50	--	1.3	0.35
49.5 ± 0.2	4	10	46.5	39	36	2.9	1.7
97.9 ± 0.3	8.5	5	94.7	41	39	4.6	2.4
147.4 ± 0.6	23.5	0.6	142.7	55 c)	40	2.1	-

a) At the entrance of the beam line to the user area.

b) At the neutron beam path at the distance of 8 m from the lithium target.

c) Upper limit due to poor energy resolution.

monitor based on counting of neutron-induced SEE is about to be installed [25]. Independent calibrations of neutron monitors are planned, using measurements of the [7]Be activity produced in the [7]Li target, following a technique suggested by Uwamino *et al.* [19].

A new upgrade of the facility is being launched in the framework of project ANITA (**A**tmospheric-like **N**eutrons from th**I**ck **TA**rget). The upgrade will allow us to deliver a neutron beam with a continuous "white" spectrum, and thus to reproduce the spectrum of neutrons in the atmosphere. Neutrons will be produced by irradiation of a thick tungsten target by high-energy protons. The possibility to deliver quasi-monoenergetic neutron beams will be kept.

Acknowledgements

References

[1] A. Koning, et al., *J. Nucl. Sci. Technol.* **2**, 1161 (2002).
[2] R. Orecchia, et al., *Eur. J. Cancer* **34**, 459 (1998).
[3] D. L. Schwartz, et al., *Int. J. Radiat. Oncol. Biol. Phys.* **50**, 449 (2001).
[4] D. T. Bartlett, et al., *Radiat. Res. Congress Proceedings* **2**, 719–723 (2000).
[5] *Single-Event Upsets in Microelectronics, topical issue,* edited by H. H. K. Tang and N. Olsson [*Mater. Res. Soc. Bull.* **28** (2003)].
[6] *JEDEC Standard. Measurements and Reporting of Alpha Particles and Terrestrial Cosmic Ray-Induced Soft Errors in Semiconductor Devices.* JESD89, August 2001.
[7] R. Nolte, et al., *Nucl. Instrum. Meth. Phys. Res. A* **476**, 369 (2002).
[8] F.P. Brady, *Can. J. Phys.* **65**, 578 (1987).
[9] H. Schuhmacher, et al., *Nucl. Instrum. Meth. Phys. Res. A* **421**, 284 (1999).
[10] N. Nakao, et al., *Nucl. Instrum. Meth. Phys. Res. A* **420**, 218 (1999).
[11] M. Baba, et al., *Nucl. Instrum. Meth. Phys. Res. A* **428**, 454 (1999).
[12] H. Condé, et al., *Nucl. Instrum. Meth. Phys. Res. A* **292**, 121 (1990).
[13] J. Klug, et al., *Nucl. Instrum. Meth. Phys. Res. A* **489**, 282 (2002).
[14] S. Dangtip, et al., *Nucl. Instrum. Meth. Phys. Res.* **A 452**, 484 (2000).
[15] S. Pomp, et al., *AIP Conf. Proc.* **769**, 780-783 (2005).
[16] S. Pomp, et al., these proceedings
[17] A.V. Prokofiev, et al., *J. Nucl. Sci. Techn., Suppl.* **2**, 112 (2002).
[18] S.G. Mashnik, et al., LANL Report LA-UR-00-1067 (2000).
[19] Y. Uwamino, et al., *Nucl. Instrum. Meth. Phys. Res. A* **389**, 463 (1997).
[20] A.N. Smirnov, et al., *Radiat. Meas.* **25**, 151 (1995).
[21] A.D. Carlson, et al., *Proc. Int. Conf. on Nuclear Data for Science and Technology, Trieste, Italy, May 19-24, 1997,* Part II, p. 1223.
[22] A.N. Smirnov, private communication.
[23] M. Olmos, private communication.
[24] I.V. Ryzhov, private communication.
[25] R. Harboe-Sorensen, private communication.